Revista Mexicana de Astronomía y Astrofísica Serie de Conferencias (RMxAC), **58**, 19–21 (2024)
© 2024: Instituto de Astronomía, Universidad Nacional Autónoma de México
https://doi.org/10.22201/ia.14052059p.2024.58.06

Stellar Feedback in the ISM. Conference Celebrating the life and work of You-Hua Chu (December 11-14, 2023)
Editors: Jesús Toló, Marfin A. Guerrero, and Guillermo M. García-Segura - DOI: https://doi.org/10.22201/ia.14052059p.2024.58.06

IMPLEMENTATION OF MULTI-ION CHEMICAL KINETICS FOR CIRCUMSTELLAR NEBULAE

Arun Mathew[1] and Jonathan Mackey[1]

RESUMEN

Se presenta el desarrollo de un módulo multi-iónico fuera de equilibrio con funciones de enfriamiento para cada ión considerando abundancias elementales arbitrarias desarrollado para cubrir un amplio rango de temperaturas entre $10^{3.5} - 10^{8.5}$ K. Se han llevado a cabo una serie de validaciones para determinar la precisión y eficiencia del módulo en diferentes escenarios, incluyendo variaciones en la temperatura, abundancias y especies químicas y en la velocidad de un flujo.

ABSTRACT

A non-equilibrium multi-ion chemistry model is developed to cover a broad temperature range of $10^{3.5} - 10^{8.5}$ K, with cooling functions computed on an ion-by-ion basis, accommodating arbitrary elemental abundances. Several validation tests are conducted to assess the accuracy and effectiveness of our approach across various scenarios, including variations in flow velocity, temperature, abundances, and chemical species.

Key Words: atomic processes — methods: numerical — plasmas — shockwaves

1. INTRODUCTION

Chemical kinetics, integrated into Hydrodynamic (HD) and Magnetohydrodynamic (MHD) simulations for investigating circumstellar nebulae around stars like Wolf-Rayet nebulae (García-Segura et al. 1996) and colliding-wind binaries (Parkin et al. 2011), often rely on oversimplified assumptions of thermal and/or ionization equilibrium or homogeneous elemental abundances. However, extreme variations in elemental abundances across circumstellar nebulae of evolved stars (Esteban et al. 2016) and the presence of strong shockwaves may invalidate these assumptions. Furthermore, in colliding-wind binaries, the winds from the two stars may exhibit vastly different abundances (e.g. Pollock et al. 2005). The application of cooling curves, whether under collisional ionization equilibrium (CIE) (e.g. Sutherland & Dopita 1993) or photoionization equilibrium (Wiersma et al. 2009), may not always be suitable in such complex scenarios. Thus, integrating more detailed models that account for these complexities may advance our understanding of the evolution of circumstellar nebulae, and certainly enables more realistic comparison of simulations with observational data on line-emission from nebulae.

In this present work, we have significantly enhanced the microphysics module within PION, a grid-based HD and MHD simulation code that includes radiative transfer of ionizing and non-ionizing photons for R-HD and R-MHD (Mackey et al. 2021). Previously, the module relied on a single tracer variable representing the Hydrogen ion fraction, with ionization states of He, C, N, and O aligned with that of hydrogen. Our new module now accommodates multiple chemical species, spatially varying elemental abundances and non-equilibrium ionization of each element. Our new module features a highly realistic ion-by-ion based cooling function utilizing CHIANTIPy v0.15.0 (Zanna et al. 2021; Young et al. 2003) with CHIANTI database version 10.0.2. This represents a significant enhancement over the previous version's cooling function.

In the forthcoming sections, we outline the theory and a comprehensive array of tests aimed at validating the accuracy and efficiency of our method across diverse scenarios. These scenarios encompass variations in density, temperature, metallicity, and chemical species. In Section 3, we establish CIE cooling functions. Additionally, we conduct 1D MHD shock tests under non-adiabatic conditions with cooling activated. Moreover, we outline our future intentions in our conclusion.

2. CHEMICAL KINETICS

Apart from the ideal inviscid MHD equations we solve the equations of all ions of H, He, C, N, O, Ne, Si, S, and Fe through

$$\frac{\partial \rho X_{\kappa,i}}{\partial t} + \nabla \cdot (\rho X_{\kappa,i} \vec{v}) = \rho S_{\kappa,i}, \qquad (1)$$

[1]Dublin Institute for Advanced Studies, Astronomy & Astrophysics Section, DIAS Dunsink Observatory, Dublin, D15 XR2R, Ireland (arun, jmackey@cp.dias.ie).

Stellar Feedback in the ISM. Conference Celebrating the life and work of You-Hua Chu (December 11-14, 2023)
Editors: Jesús Toló, Marfin A. Guerrero, and Guillermo M. García-Segura - DOI: https://doi.org/10.22201/ia.14052059p.2024.58.06

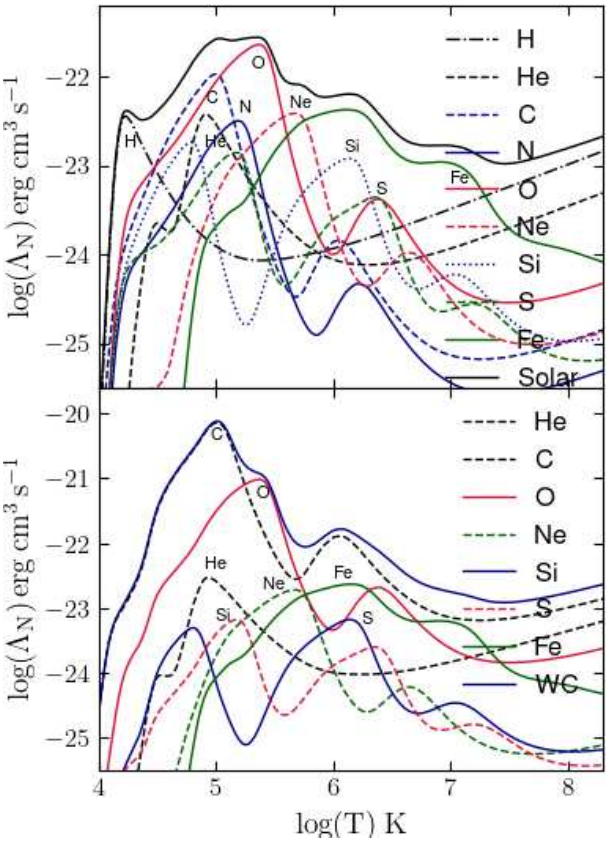

Fig. 1. Elemental contributions $n_e \sum_i n_{\kappa,i}\,\Lambda_{\kappa,i}$ (scaled with $(m_H/\rho)^2$) and net cooling function $\Lambda_{\rm N}$ for Solar (top panel) and WC (bottom panel) abundances.

where $X_{\kappa,i}$ denotes the fraction of the i-th ionization state of element κ. The source term $S_{\kappa,i}$ represents the net rate of change due to ionization processes, given by:

$$S_{\kappa,i} = X_{\kappa,i+1} n_e \alpha_{\kappa,i+1} - X_{\kappa,i}\,(n_e \zeta_{\kappa,i} + n_e \alpha_{\kappa,i} + \beta \delta_{i0}) + X_{\kappa,i-1} n_e \zeta_{\kappa,i-1}, \quad (2)$$

where, $\zeta_{\kappa,i}(T)$ and $\alpha_{\kappa,i}(T)$ are temperature-dependent collisional ionization and recombination rate coefficients, respectively. The cosmic-ray ionization rate is assumed constant at $\beta = 1.0 \times 10^{-17}$ s^{-1} (Goldsmith & Langer 1978) and δ_{i0} is the Kronecker delta. These equations are solved using an operator splitting method, with the source term evolved using backward differencing with Newton iteration utilizing the SUNDIALS/CVODE library (Cohen et al. 1996).

The source term for the energy equation associated with chemical kinetics is

$$S_E = -(L_{\rm coll} + L_{\rm rec} + L_{\rm cool}) + Q_{\rm cr}\,, \quad (3)$$

with the radiative cooling term given by $L_{\rm cool} = n_e \sum_{\kappa,i} n_{\kappa,i}\,\Lambda_{\kappa,i}$, involving individual radiative cooling rates $\Lambda_{\kappa,i}(n_e, T)$ per electron, per ion of the species κ, and charge i, calculated using CHIANTIPy v0.15.0 with CHIANTI database version 10.0.2. Radiative losses due to recombination are expressed as $L_{\rm rec} = \frac{3}{2} k_{\rm B} n_e T \sum_\kappa \sum_{i=1}^{N_\kappa} \alpha_{\kappa,i} n_{\kappa,i}$, and radiative losses due to collisional processes are given by $L_{\rm coll} = n_e \sum_\kappa \sum_{i=0}^{N_\kappa - 1} I_{\kappa,i} \zeta_{\kappa,i} n_{\kappa,i}$. The heating consists of cosmic rays and is represented by $Q_{\rm cr} = \langle E_{\rm cr} \rangle\, \beta \sum_\kappa n_{\kappa,0}$. This is based on the simple assumption of constant deposition of average ionization energy, with $\langle E_{\rm cr} \rangle = 20$ eV per ionization of neutral species into the gas. The source term is evaluated by integrating the internal energy density of the gas together with the ionization rate equations in CVODE.

3. SIMULATIONS AND RESULTS

PION is now updated to include cooling rates for a range of ions including H, He, C, N, O, Ne, Si, S, and Fe. We compute the ionization fraction for all ions corresponding to the aforementioned elements under CIE, as a function of temperature. Utilizing this one can obtain the CIE cooling function as shown in Figure 1. Here the radiative cooling accounts for line-emission, free-bound emission, Bremsstrahlung emission, and two-photon emission.

The top panel of Figure 1 depicts cooling contributions from various elements under CIE conditions at different temperatures, assuming solar photospheric abundances (Asplund et al. 2009). These align with prior computations (Sutherland & Dopita 1993), though differences in atomic data can cause variations. The bottom panel contrasts the cooling function obtained for a plasma with abundances appropriate for the wind of a WC9 star (Eatson et al. 2022), where cooling is notably higher compared to solar abundances, particularly in the range $\log T$ from 4.5 to 6.5. However, in the $10^4 < T < 1.5 \times 10^4$ K range, solar abundances exhibit superior cooling, emphasizing the impact of elemental abundances on cooling.

Figure 2 depicts the spatial ionization profile of Fe in a non-adiabatic planar shock test with inflow velocities of 1000 km/s and 3000 km/s. The flow direction is from right to left, and the shock is located near the right edge of the plot. Ionization progresses from right to left starting from the shock front, due to finite ionization time scales for each ionization state. The temperature increase behind the shock allows ionization across multiple Fe ion levels. Higher ionization states become significant at specific distances from the shock front, influenced by the gas

Stellar Feedback in the ISM. Conference Celebrating the life and work of You-Hua Chu (December 11-14, 2023)
Editors: Jesús Toló, Marfin A. Guerrero, and Guillermo M. García-Segura - DOI: https://doi.org/10.22201/ia.14052059p.2024.58.06

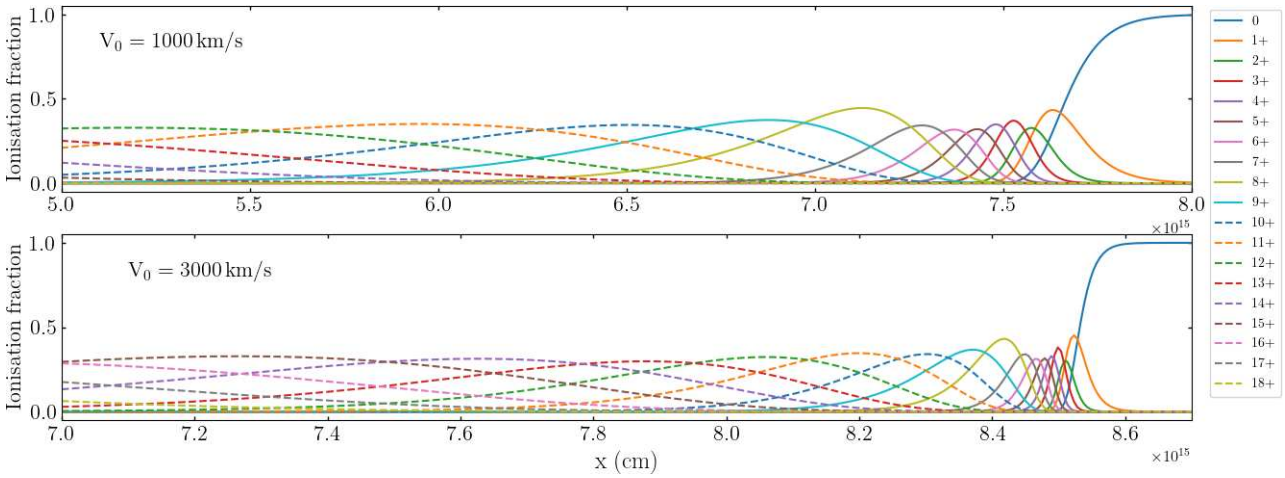

Fig. 2. Spatial profiles of ion fractions for different ionization levels of Iron behind the shock front in non-adiabatic flows at velocities of 1000 km/s (top panel) and 3000 km/s (bottom panel).

temperature. Immediately behind the shock, lower ionization states dominate the emission spectra, albeit with minor contributions due to their smaller area under the curve. In contrast, highly ionized gas emits away from the shock front, contributing substantially to the spectra. However, as the post-shock gas cools, recombination processes promote increasing contributions from lower ionization states to the spectra.

4. CONCLUSION

Here, we introduce a novel non-equilibrium multi-ion module being developed for the R-MHD code PION. This provides enhanced accuracy in tracking ionization state and temperature both temporally and spatially. This advancement holds significant promise for enhancing the predictive capabilities of computer simulations. For instance, it can greatly improve the fidelity of synthetic X-ray spectra of hot plasma and the spectral lines of ions across UV/optical/IR wavelengths. Moreover, the incorporation of an ion-by-ion cooling function further strengthens its utility, enabling meaningful predictions even under non-equilibrium conditions where elemental abundances may dynamically evolve, such as in scenarios involving stellar wind or colliding-wind binaries.

Our future plans involve expanding this module's functionality to encompass multi-ion photoionization resulting from a single radiation source and charge exchange reactions. This extension will broaden the scope of applications, enabling more comprehensive simulations in scenarios where such interactions play a crucial role.

REFERENCES

Asplund, M., Grevesse, N., Sauval, A. J., & Scott, P. 2009, ARA&A, 47, 481, https://doi.org/10.1146/annurev.astro.46.060407.145222

Cohen, S. D., Hindmarsh, A. C., & Dubois, P. F. 1996, ComPh, 10, 138, https://doi.org/10.1063/1.4822377

Eatson, J. W., Pittard, J. M., & Van Loo, S. 2022, MNRAS, 516, 6132, https://doi.org/10.1093/mnras/stac2617

Esteban, C., Mesa-Delgado, A., Morisset, C., & García-Rojas, J. 2016, MNRAS, 460, 4038, https://doi.org/10.1093/mnras/stw1243

García-Segura, G., Langer, N., & Mac Low, M. 1996, A&A, 316, 133

Goldsmith, P. F. & Langer, W. D. 1978, ApJ, 222, 881

Mackey, J., Green, S., Moutzouri, M., et al. 2021, MNRAS, 504, 983

Parkin, E. R., Pittard, J. M., Corcoran, M. F., & Hamaguchi, K. 2011, ApJ, 726, 105

Pollock, A. M. T., Corcoran, M. F., Stevens, I. R., & Williams, P. M. 2005, ApJ, 629, 482

Sutherland, R. S. & Dopita, M. A. 1993, ApJS, 88, 253

Wiersma, R. P. C., Schaye, J., & Smith, B. D. 2009, MNRAS, 393, 99

Young, P. R., Del Zanna, G., Landi, E., et al. 2003, ApJS, 144, 135

Del Zanna, G., Dere, K. P., Young, P. R., & Landi, E. 2021, ApJ, 909, 38, https://dx.doi.org/10.3847/1538-4357/abd8ce